Hindawi
Advances in Materials Science and Engineering
Volume 2019, Article ID 1261694, 8 pages
https://doi.org/10.1155/2019/1261694

Research Article

Experimental Study on Mechanical Behavior of a New Backfilling Material: Cement-Treated Marine Clay

Nan Zhou[1], **Shenyang Ouyang**[1], **Qiangqiang Cheng**[1,2] and **Feng Ju**[3]

[1]*State Key Laboratory of Coal Resources and Safe Mining, China University of Mining & Technology, Xuzhou 221116, China*
[2]*Jiangsu Vocational Institute of Architectural Technology, Xuzhou 221116, China*
[3]*State Key Laboratory for Geomechanics and Deep Underground Engineering, China University of Mining & Technology, Xuzhou 221116, China*

Correspondence should be addressed to Qiangqiang Cheng; qiangcheng@cumt.edu.cn

Received 10 December 2018; Accepted 2 February 2019; Published 14 March 2019

Academic Editor: Hossein Moayedi

Backfilling mining method is an overlying strata control way, which is widely used in underground coal mine. This method is effective in preventing and controlling geological disasters such as surface subsidence, mine water inrush, rock burst, and other disasters. Cement-treated marine clay (CMC) is a typical porous media, which has abundant reserves and can be used as a new backfilling material. Therefore, the mechanical characteristics of CMC are very important for overlying strata control in coal mine. To investigate stress-strain behavior of CMC, isotropic consolidated drained (CID) triaxial test and isotropic compression test (ICT) were conducted with different confining pressures in the range of 50–800 kPa. Stress-strain behavior was found similar to those of the overconsolidated stress-strain behavior as well as the pore water pressure versus strain. Stress versus strain curves under lower confining pressure 50–250 kPa presented shear dilatancy. The result shows that the peak strength increased linearly with increasing confining pressure. The internal friction angle and cohesion are 48° and 590 kPa, respectively. Before the confining pressure reaches 727 kPa, which is the primary yielding point, the secant modulus E_1 (the secant modulus at 1% axial strain) and the secant modulus E_{50} (corresponding to the 50% of the peak point) increase initially and decrease afterwards with the increasing of confining pressure. Afterwards, the two parameters increased with increasing confining pressure. The yielding stress occurred in the stage, generating a dramatic decrease in tangent modulus. This study can be a theoretical basis for engineering application of this new backfilling material.

1. Introduction

In underground mining, the stress balance of stope is destroyed as a result of overlying strata moving and fracturing. The overlying strata rupture at the gob, and "three zones" were formed from coal seam to upper strata, which are named caving zone, fractured zone, and bending zone, respectively. The rupture of overlying strata usually leads to disasters such as mine water inrush, rock burst, gas outburst, surface subsidence, and other disasters (Figure 1). Backfilling mining method is widely used in underground coal mine for overlying strata control, and the overlying strata are supported by solid backfilling materials (Figure 2). This mining method effectively prevents the rupture of overlying strata and then decreases the geological disasters in mine [1, 2]. The support ability of backfilling body depends on the mechanical characteristics of materials [3], which are usually composed of gangue, fly ash, tailings, or limes. Wu et al. [4] studied thermal, hydraulic, and mechanical performances of cemented coal gangue-fly ash backfill. Deng et al. [5, 6] developed a new type of CPB with waste rock as coarse aggregate, fly ash as fine powder, slag as activator, and ordinary Portland cement as binder. Niroshan et al. [7] studied relationship of the microstructure and long-term mechanical properties of the cemented filling material. De Araújo et al. [8] studied the shear strength of a cemented paste backfill under high confining pressure condition. Yilmaz and Fall proposed that the mechanical characteristics of tailing paste backfilling materials are influenced by chemical and physical factors [9].

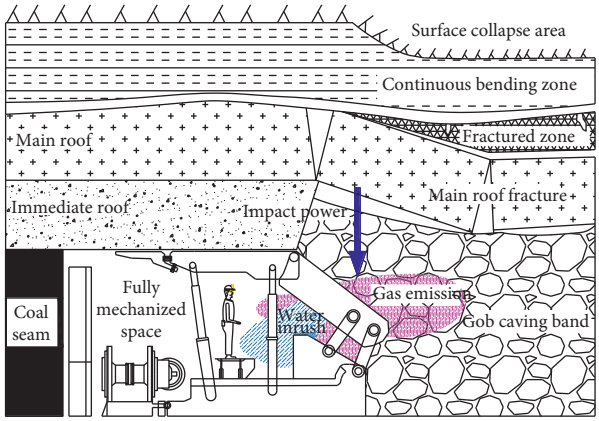

Figure 1: Traditional working face.

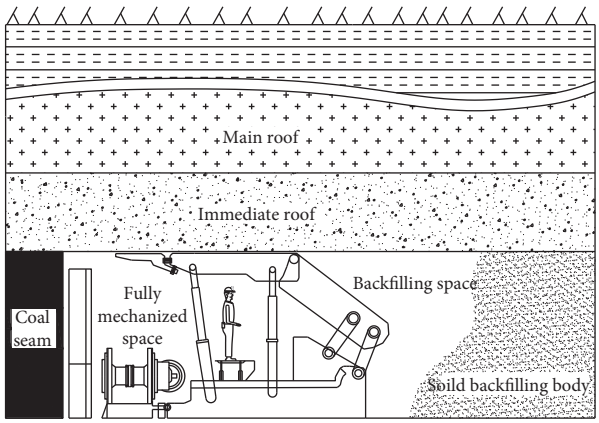

Figure 2: Solid backfilling mine working face.

Marine clays are composite materials that include fine sand and clay and rich in calcareous and siliceous sediments. In general, marine clays are soft cemented and have the characteristics of soft sensitive and highly compressive [10]. Marine clays have abundant reserve in the offshore area, and they can be used as backfilling materials in the mine located on the coastal region. As a backfilling material, the mechanical characteristics of marine clays are changing with increasing of mine depth, which caused by different confined stresses. Thus, it is important to study the mechanical characteristics of marine clay under different confined stresses because it determines the control effect of overlying strata. Compared to other chemical stabilization methods, using cement to improve the strength of soft clay is a popular solution because cementation can cause formation of weak to strong bonds between soil particles, as well as it is more economic and effective for subgrade engineering, embankments, deep excavation, and underground construction. Selection criteria for the choice of a particular cementing agent for soil improvement include factors such as increase in density, strength (primarily the unconfined compressive strength), and durability. Shear strength of cemented soils is one of the most important parameters in geotechnical engineering. Many researchers have investigated unconfined compressive strength q_u of cement-stabilized clay [11, 12]. Several studies have been conducted on the tensile strength of cement-improved clay [13, 14]. The physical-chemical and microstructural aspects of cement-treated Singapore marine clay have been studied [15]. Some researchers have examined the isotropic compression and the undrained shear behavior of cement-treated soils [16–19]. Very little attention has been given to the influence of confining pressure on the overall mechanical behavior [20, 21].

This paper presents a study on effect of the primary yielding confining pressure on shear characteristics of CMC by using the drained triaxial test and isotropic compression test, including stress-strain behavior, volume-strain relationship, pore water-strain relationship, shear strength behavior, failure modes, and deformation behavior. It is important to the engineering design of marine clay materials backfilling method.

Table 1: Physical characteristics of Singapore marine clay [22].

	Values
Soil characteristics	
Specific gravity (Mg/m^3)	2.70
Liquid limit (%)	74.07
Plastic limit (%)	31.00
Plasticity index (%)	43.07
Particle size	
Colloid (% < 1 μm)	24.1
Clay (% < 4 μm)	21.8
Silt (4 μm < % < 62.5 μm)	47.7
Fine sand (62.5 μm < % < 250 μm)	6.2
Medium sand (250 μm < % < 500 μm)	0.2

Table 2: Chemical compositions of OPC by weight (%) [22].

Chemical composition	OPC
Silica, SiO_2	20.61
Alumina, Al_2O_3	4.89
Ferric oxide, Fe_2O_3	3.4
Magnesium oxide, MgO	2.48
Sulfur oxide, SO_3	2.08
Potassium oxide, $K_2O + Na_2O$	0.3
Calcium oxide, CaO	65.04

2. Materials and Experimental Methodology

2.1. Materials. The studied materials include Singapore upper marine clay and ordinary Portland cement (OPC), the type of which is 42.5R. The main physical characteristics of the marine clay are presented in Table 1.

The liquid limit and plastic limit of marine clay are, respectively, 74.07 and 31.00%, which indicates that the plasticity index of 43.07%. The constituents of marine clay are approximately 24.1% colloid, 21.8% clay, 47.7% silt, 6.2% fine sand, and 0.2% medium sand. Table 2 shows the chemical compositions of OPC by weight. In addition, the organic content of this soil is less than 1%, in which effect on the mechanical test can be neglected.

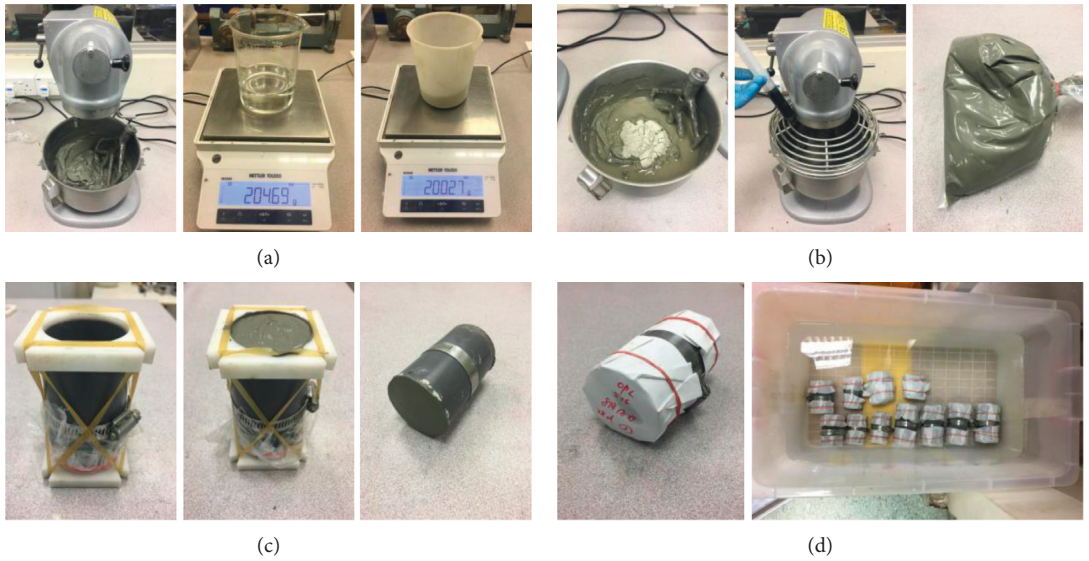

Figure 3: Specimen preparation procedure.

Table 3: Basic parameters of samples tested.

Test ID	Confining pressure (kPa)	Number of specimens	Sample diameter × sample height (mm × mm)	The quality in the air (g)	The quality in the water (g)	Density (g/cm^3)	Average peak strength p_p (kPa)
1	50	2	38.00 × 76.00	128.0	42.8	1.486	1201.1
2	200	1	37.93 × 76.09	127.9	42.1	1.488	1385.8
3	250	1	37.98 × 76.04	128.1	42.6	1.488	1448.1
4	350	1	38.00 × 76.00	127.9	41.9	1.485	1779.3
5	500	1	38.02 × 76.12	128.2	42.4	1.484	1822.8
6	600	1	37.91 × 76.00	128.4	42.1	1.498	2080.1
7	800	1	38.00 × 76.00	128.6	42.3	1.493	2760.0
8	ICT*	2	37.94 × 76.06	128.4	42.0	1.490	—

Note: tests 1–7 are isotropic consolidated drained (CID) tests; *test 8 is the isotropic compression test (ICT) for primary yield stress.

2.2. Sample Preparation and Testing. The mix ratio of CMC studied is 213, and the curing time is 28 days. The mix ratio 213 means that the mass ratio value of dry soil solid (S): dry cement solid (C): water (W) is 2 : 1 : 3 [23]. The mix ratio 213 was used in several cement clay stabilization researches, such as deep mixing and jet-grouting studies and projects including soft, fine-grained soils [24, 25].

The main procedure of sample preparation is the same with that used by Chin et al. [26]. It has been noted by Kamon that clay particles are aggregated with average diameter of up to 60 mm (0.05–0.6 mm) [27]. The first step was to use a sieve size of 0.3 mm filter to ensure the homogeneity of the clay after soaking in water for days and clearing its small rocks, pebbles, sea shells, etc. Then, the marine clay was first mixed in a Hobart mixer for 5 minutes and then added the prescribed amount of water to achieve 100% moisture content for another 5 minutes; after which, both cement and water left according to the desired ratio 213 were added to the Hobart mixer and mixed for 10 minutes. And then, the mixed soils were removed and stored in a plastic bag to preserve the water content and to ensure the fixed environment atmosphere. Later, the prepared mixture was placed into the prepared molds, which diameter is 38 mm and height is 76 mm. Finally, the specimens were labeled and stored in a PVC box which contains distilled water. It should be noted that all samples should be completed within half an hour. Figure 3 shows the whole specimen preparation procedure. Table 3 presents the basic parameters of samples tested in this study. The confining pressure was maintained in the range 50–800 kPa.

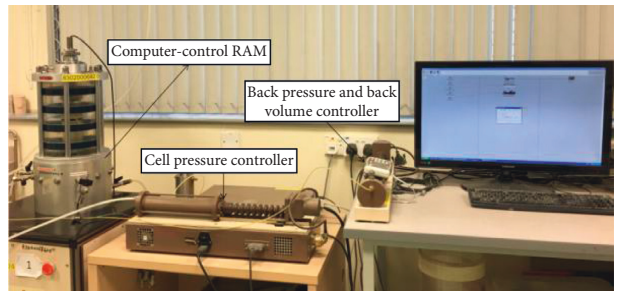

Figure 4: GDS controlled by computer in the CID test.

The treated marine clay specimens were tested using isotropic consolidated and drained triaxial test, consolidation test, and constant stress ratio test. The triaxial GDS equipment is a fully computer controlled triaxial stress path equipment, as shown in Figure 4.

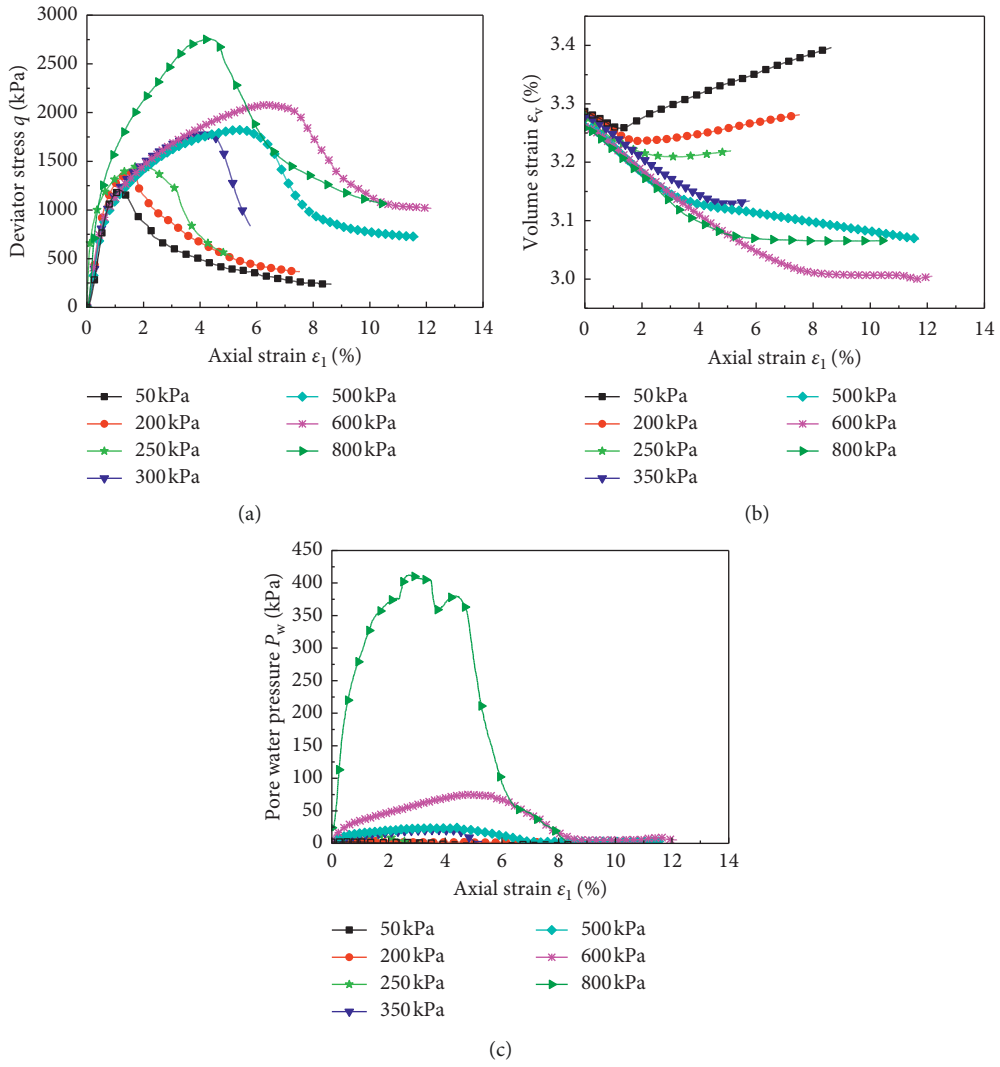

Figure 5: Curves of (a) deviator stress-axial strain, (b)volume strain-axial strain, and (c) pore water pressure-axial strain with different confining pressures.

The mechanical test used a back pressure of 500 kPa, and the B-value reached at least 0.95. The vertical consolidation force and the shear force were designed as follows: 50, 200, 250, 350, 500, 600, and 800 kPa. It should be noted that the primary yielding pressure is 727 kPa, and therefore, the maximum loading force is 800 kPa. Since shearing and friction effect are negligible to the pore pressure changes, a shearing rate of 0.005 mm/min was selected to ensure the pore pressure changes, which was demonstrated to be true by the tests results [26, 28].

Isotropic compression procedures followed the prescribed procedures in ISO/TS 17892-9 [29, 30]. It was done by using a high-pressure test system supplied by GDS, as shown in Figure 4. The sample was saturated under back pressure until the B-value approached at least 0.9 [31], which requires a back pressure of 400 kPa approximately. This test used back pressure of 500 kPa, and the B-value reached at least 0.95. Consolidation and swelling were conducted at a stress rate of 1 kPa/min with side drainage.

3. Results and Discussion

3.1. Stress-Strain Behavior. Figure 5 presents the curves of the axial strain ε_1-q-ε_v-pore pressure with different confining pressures in the range of 50–800 kPa of the CMC with the mix ratio 213 as well as the curing time 28 days. All stress-strain curves show an apparent peak point, which increases obviously with the increasing confining pressure. The stress deceases quickly after reaching the peak point. The curves are similar to those of the overconsolidated stress-strain curves, which are all smooth hump shapes, showing a plastic failure (Figure 5(a)). The stress-strain behavior is approximately the same with that tested by Haeri et al. [32] and Hao et al. [33, 34].

When the confining pressure is lower, e.g., 50–250 kPa, ε_1-ε_v relationship can be expressed as dilatancy; however, other under higher confining pressure conditions show an opposite trend. As the confining pressure increases, the dilation increases because of the reduction in the brittleness in the cemented soils (Figure 5(b)).

As indicated in Figure 5(c), the pore water pressure curves present a nonlinear increasing trend with increasing confining pressure. The pore water pressure reaches to the peak when the responding deviator stress reaches to the peak. It can be concluded that the main trend of deviator stress-axial strain and pore water pressure-axial strain is similar. Pore water pressure changes little under 500 kPa or lower than it, but it increases obviously when the confining pressure is more than 500 kPa, which can reach as high as 430 kPa during the shearing procedure. Pore water pressure is equal to the primary point at the beginning of the shear test, which is constant after axial strain reached approximately 10%, no matter what confining pressures.

3.2. Shear Strength Behavior. According to the drained test results, the peak strength under different confining pressures was sorted out, as shown in Figure 6. The peak strength p_p increases linearly with increasing confining pressure σ_3 and can be fitted well by the following straight line:

$$p_p = 1.981\sigma_3 + 1003.6. \quad (1)$$

According to the test results, Mohr circles at failure and strength envelopes are compiled in Figure 7. As shown in Figure 7, the internal friction angle and cohesion are 48° and 590 kPa, respectively, though under different confining pressures. The internal friction angle of CMC is approximately 2.2 times than that of without cement [25]. Actual shear damage angle and destruction modes in the test are listed in Table 4, which can be drawn from Figure 8. The average actual shear damage angle is approximately 55°. The failure modes of CMC are basically the same, with a shear zone; the stress-strain curves are strain-softening type (Figure 8).

3.3. Deformation Behavior. In order to study the effect of confining pressure on the deformation properties of cement-treated soils, the secant modulus E_1 (the secant modulus at 1% axial strain) and the secant modulus E_{50} (corresponding to the 50% of the peak point) are shown in Figure 9. Before the confining pressure reaches 727 kPa, which is the primary yielding point, the secant modulus E_1 and the secant modulus E_{50} increase initially and decrease afterwards with the increasing of confining pressure. Afterwards, the two parameters increased with increasing confining pressure.

To research more in-depth, the isotropic compression test has been conducted to find the yielding point. As shown in Figure 10, the isotropic compression curve of OPC showed significant linear pre- and postyield segments, which allow its recompression and compression indices to be determined. This is consistent with the linear v-lnp' relationship assumed by Ghee [35] and Xiao and Lee [36]. The isotropic yielding stress is defined as the point where the

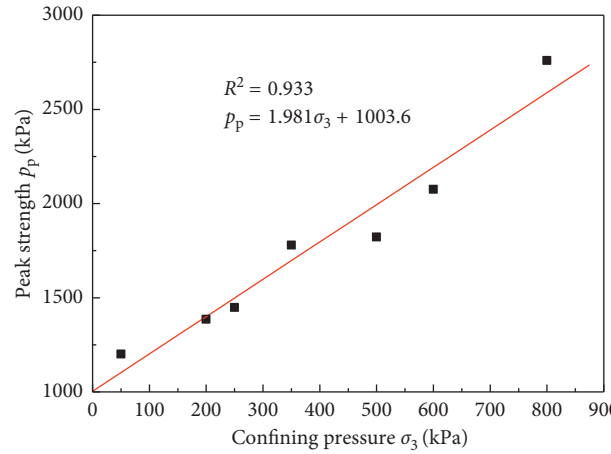

Figure 6: Relationship between confining pressure and peak strength.

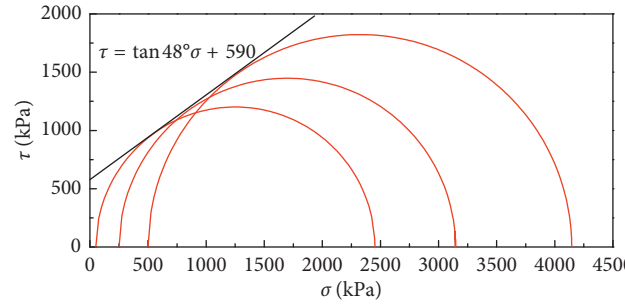

Figure 7: Mohr circles at failure and strength envelopes.

Table 4: Actual shear damage angle.

Confining pressure (kPa)	50	200	250	350	500	600	800
Actual shear angle (degrees)	56	65	40	54	55	56	58

compression curve starts to deviate from the initial linear behavior under a natural coordinate system [12, 37]. The yield stress was determined by best fitting a straight line with the initial part of the compression curve on the compression space by trial and error [23]. The yielding stress occurs in the stage, generating a dramatic decrease in tangent modulus. Also, the yielding stress point of cement-treated soils in the test is approximately 727 kPa, and the changing trend of secant moduli E_1 and E_{50} is nearly the same with conclusions by Wang et al. [38].

4. Conclusions

In order to investigate the influence of primary yielding stress on the mechanical characteristics of CMC, the isotropic consolidated drained triaxial test and isotropic compression test were conducted with different confining pressures in the range of 50–800 kPa. The stress-strain behavior, shear strength, and deformation behavior are studied in this paper. The following conclusions can be drawn according to the test results:

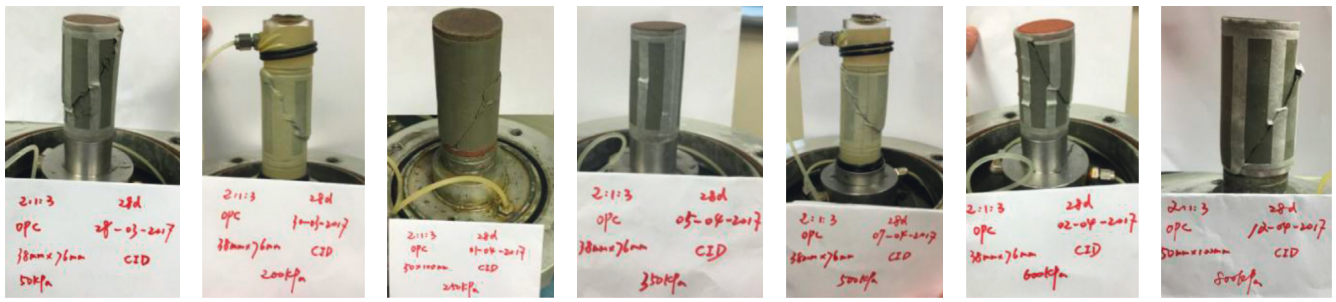

(a) (b) (c) (d) (e) (f) (g)

Figure 8: Failure modes with different confining pressures (σ_3) [22]. (a) $\sigma_3 = 50$ kPa. (b) $\sigma_3 = 200$ kPa. (c) $\sigma_3 = 250$ kPa. (d) $\sigma_3 = 350$ kPa. (e) $\sigma_3 = 500$ kPa. (f) $\sigma_3 = 600$ kPa. (g) $\sigma_3 = 800$ kPa.

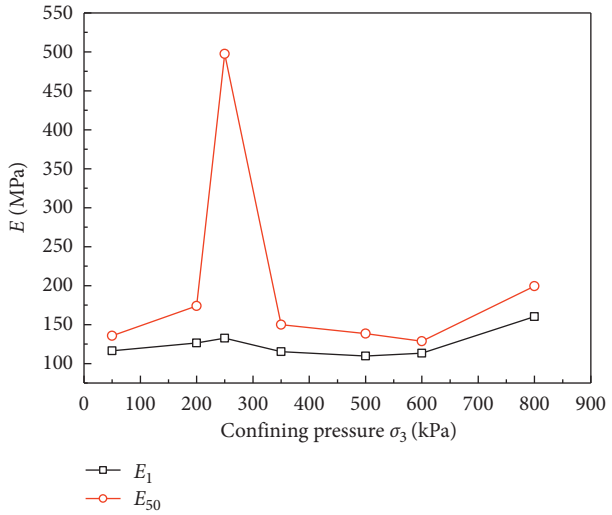

Figure 9: Relationship between confining pressure and E (E_1 and E_{50}).

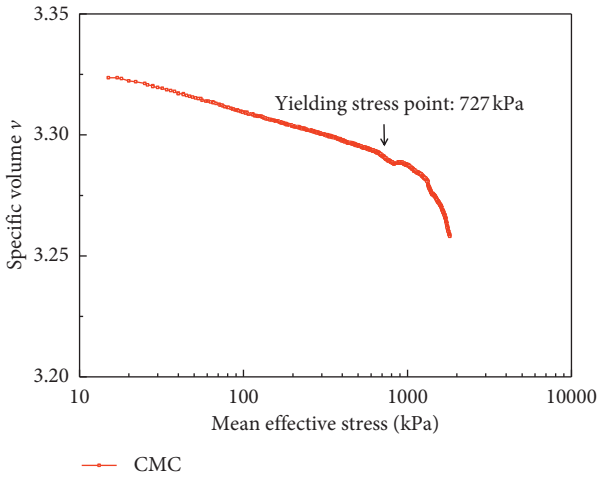

Figure 10: Mean effective stress versus specific volume of CMC.

(1) The brittleness in the CMC reduces as the confining pressure increases. Nonlinear stress-strain behavior shows similarity to the overconsolidated stress-strain trend, both of which have an apparent peak point, increase obviously with the increasing confining pressure, and are smooth hump shapes, showing a plastic failure. Pore water pressure-axial strain is similar to that of deviator stress-axial strain, which is constant after axial strain reached approximately 10%, no matter what confining pressures.

(2) The shear strength of OPC stabilized marine clay increases when confining pressure increases. The peak shear strength can be fitted well by the straight line $p_p = 1.981\sigma_3 + 1003.6$ kPa, as well as the fitting parameter $R^2 = 0.933$, which applies to the range of confining pressure applied in this study. The internal friction angle and cohesion are 48° and 590 kPa, respectively. The failure modes of CMC, with a shear zone, are strain-softening types.

(3) Significant linear pre- and postyield segments can be drawn by the isotropic compression, which allow its recompression and compression indices to be determined. The yield stress 727 kPa approximately is determined by best fitting a straight line with the initial part of the compression curve on the compression space by trial and error.

(4) Both the secant moduli E_1 and E_{50} have an increasing, then decreasing trend till to the primary yielding stress point 727 kPa and at last increasing trend with increasing confining pressure. To CMC, the primary yielding occurs in the stage, generating a dramatic decrease in tangent modulus.

This study can be a theoretical basis for the engineering application of the marine clay backfilling material. And the further study should focus on the influences of primary yielding confining stress on micromechanical behavior of the CMC.

Data Availability

The data used to support the findings of this study are included within the article.

Conflicts of Interest

The authors declare that there are no conflicts of interest regarding the publication of this paper.

Acknowledgments

The authors gratefully acknowledge the support provided by the National University of Singapore, the Prof. and Dr. special subject funds for Jiangsu Vocational Institute of Architectural Technology (no. JYBZX18-02), Ministry of Housing and Urban Science and Technology Program (2018-K7-004), Jiangsu Provincial Housing and Construction Department Science and Technology Plan (2018ZD021), 2018 Qinglan Project in Jiangsu Province and 2017 Jiangsu Provincial, Higher School Natural Science Research Major Project (17KJA560002). The Research Fund of the State Key Laboratory of Coal Resources and Safe Mining, CUMT (SKLCRSM19KF012), is gratefully acknowledged.

References

[1] J. Zhang, Q. Zhang, A. J. S. Spearing, X. Miao, S. Guo, and Q. Sun, "Green coal mining technique integrating mining-dressing-gas draining-backfilling-mining," *International Journal of Mining Science and Technology*, vol. 27, no. 1, pp. 17–27, 2017.

[2] P. Huang, A. J. S. Spearing, J. Feng, K. V. Jessu, and S. Guo, "Effects of solid backfilling on overburden strata movement in shallow depth longwall coal mines in West China," *Journal of Geophysics and Engineering*, vol. 15, no. 5, pp. 2194–2208, 2018.

[3] N. Zhou, Q. Zhang, F. Ju, and S. Liu, "Pre-treatment research in solid backfill material in fully mechanized backfilling coal mining Technology," *Disaster Advances*, vol. 6, pp. 118–125, 2013.

[4] D. Wu, Y. Hou, T. Deng, Y. Chen, and X. Zhao, "Thermal, hydraulic and mechanical performances of cemented coal gangue-fly ash backfill," *International Journal of Mineral Processing*, vol. 162, pp. 12–18, 2017.

[5] X. Deng, J. Zhang, B. Klein, N. Zhou, and B. deWit, "Experimental characterization of the influence of solid components on the rheological and mechanical properties of cemented paste backfill," *International Journal of Mineral Processing*, vol. 168, pp. 116–125, 2017.

[6] X. Deng, B. Klein, L. Tong, and B. de Wit, "Experimental study on the rheological behavior of ultra-fine cemented backfill," *Construction and Building Materials*, vol. 158, pp. 985–994, 2018.

[7] N. Niroshan, L. Yin, N. Sivakugan, and L. V. Ryan, "Relevance of sem to long-term mechanical properties of cemented paste backfill," *Geotechnical and Geological Engineering*, vol. 36, no. 4, pp. 2171–2187, 2018.

[8] E. E. B. De Araújo, F. A. N. de França, D. Simon, N. O. De Freitas, and O. Francisco Dos Santos, "Shear strength of a cemented paste backfill submitted to high confining pressure," *Applied Mechanics and Materials*, vol. 858, pp. 219–224, 2017.

[9] E. Yilmaz and M. Fall, *Paste Tailings Management*, Springer, Berlin, Germany, 2017.

[10] A. Nader, M. Fall, and R. Hache, "Characterization of sensitive marine clays by using cone and ball penetrometers: example of clays in eastern Canada," *Geotechnical & Geological Engineering*, vol. 33, no. 4, pp. 841–864, 2015.

[11] S. C. Chian, S. T. Nguyen, and K. K. Phoon, "Extended strength development model of cement-treated clay," *Journal of Geotechnical and Geoenvironmental Engineering*, vol. 142, no. 2, article 06015014, 2016.

[12] H. Xiao, F. H. Lee, and K. G. Chin, "Yielding of cement-treated marine clay," *Soils and Foundations*, vol. 54, no. 3, pp. 488–501, 2014.

[13] Y. T. Pan, H. W. Xiao, F. H. Lee, and K. K. Phoon, "Modified isotropic compression relationship for cement-admixed marine clay at low confining stress," *Geotechnical Testing Journal*, vol. 39, no. 4, article 20150147, 2016.

[14] S. H. Liang, M. Wang, L. Zhang, S. Z. Zhou, and Y. F. Zhang, "Experimental study of mechanical properties and microstructures on nansha soft soil stabilised with cement," *Materials Research Innovations*, vol. 19, no. 8, pp. S8-518–S8-524, 2016.

[15] S. K. Bharati and S. H. Chew, "Geotechnical behavior of recycled copper slag-cement-treated Singapore marine clay," *Geotechnical and Geological Engineering*, vol. 34, no. 3, pp. 835–845, 2016.

[16] F. Oka and S. Kimoto, "A cyclic elastoplastic constitutive model and effect of non-associativity on the response of liquefiable sandy soils," *Acta Geotechnica*, vol. 13, no. 6, pp. 1283–1297, 2018.

[17] L. Cui and M. Fall, "An evolutive elasto-plastic model for cemented paste backfill," *Computers and Geotechnics*, vol. 71, pp. 19–29, 2016.

[18] A. Dehghan and A. Hamidi, "Triaxial shear behaviour of sand-gravel mixtures reinforced with cement and fibre," *International Journal of Geotechnical Engineering*, vol. 10, no. 5, pp. 510–520, 2016.

[19] S. De'An and H. Matsuoka, "An elastoplastic model for frictional and cohesive materials and its application to cemented sands," *International Journal for Numerical & Analytical Methods in Geomechanics*, vol. 4, no. 6, pp. 525–543, 2015.

[20] V. Favero, A. Ferrari, and L. Laloui, "Anisotropic behaviour of opalinus clay through consolidated and drained triaxial testing in saturated conditions," *Rock Mechanics and Rock Engineering*, vol. 51, no. 5, pp. 1305–1319, 2018.

[21] A. Taheri and F. Tatsuoka, "Small- and large-strain behaviour of a cement-treated soil during various loading histories and testing conditions," *Acta Geotechnica*, vol. 10, no. 1, pp. 131–155, 2015.

[22] Q. Cheng, K. Yao, and Y. Liu, "Stress-dependent behavior of marine clay admixed with fly-ash-blended cement," *International Journal of Pavement Research and Technology*, vol. 11, no. 6, pp. 611–616, 2018.

[23] H. Xiao, "Evaluating the stiffness of chemically stabilized marine clay," *Marine Georesources & Geotechnology*, vol. 35, no. 5, pp. 698–709, 2017.

[24] F.-H. Lee, Y. Lee, S.-H. Chew, and K.-Y. Yong, "Strength and modulus of marine clay-cement mixes," *Journal of Geotechnical and Geoenvironmental Engineering*, vol. 131, no. 2, pp. 178–186, 2005.

[25] H. Xiao, *Yielding and failure of cement treated soil*, Ph.D. thesis, National University of Singapore, Singapore, 2009.

[26] K. G. Chin, F. H. Lee, and G. R. Dasari, "Effects of curing stress on mechanical properties of cement-treated soft marine clay," in *Proceedings of the International Symposium on Engineering Practice and Performance of Soft Deposits*, pp. 217–222, Osaka, Japan, June 2004.

[27] M. Kamon, "Design and performance criteria for methods of precompression and speeding of consolidation other than vertical drains," in *Proceedings of VIII ECSMFE*, Helsinki, Finland, 1983.

[28] Q. Cheng, H. Xiao, Y. Liu, W. Wang, and L. Jia, "Primary yielding locus of cement-stabilized marine clay and its

applications," *Marine Georesources & Geotechnology*, vol. 22, no. 2, pp. 1–18, 2018.

[29] I. O. f. Standardization, *Geotechnical Investigation and Testing-Laboratory Testing of Soil. Part 7*, International Organization for Standardization, Geneva, Switzerland, 2004.

[30] I. O. f. Standardization, *Geotechnical Investigation and Testing-Laboratory Testing of Soil. Part 9*, International Organization for Standardization, Geneva, Switzerland, 2004.

[31] N. Li, J. Chang, C. Jiang et al., "Unstart/restart hysteresis characteristics analysis of an over-under TBCC inlet caused by backpressure and splitter," *Aerospace Science and Technology*, vol. 72, pp. 418–425, 2018.

[32] S. M. Haeri, A. Hamidi, S. M. Hosseini, E. Asghari, and D. G. Toll, "Effect of cement type on the mechanical behavior of a gravely sand," *Geotechnical and Geological Engineering*, vol. 24, no. 2, pp. 335–360, 2006.

[33] J. Hao, "Discussion of the ideal mechanical feature for cement-soil," *Chinese Journal of Geotechnical Engineering*, vol. 13, no. 3, pp. 53–59, 1991.

[34] Z. Liu, J. G. Zhu, and H. Liu, "Experimental study of cemented gravelly soil by triaxial test," *Rock & Soil Mechanics*, vol. 33, no. 7, pp. 2013–2020, 2012.

[35] C. K. Ghee, "Constitutive behaviour of cement treated marine clay," Ph.D. thesis, National University of Singapore, Singapore, 2006.

[36] H.-W. Xiao and F.-H. Lee, "An energy-based isotropic compression relation for cement-admixed soft clay," *Géotechnique*, vol. 64, no. 5, pp. 412–418, 2014.

[37] G. V. Rotta, N. C. Consoli, P. D. M. Prietto, M. R. Coop, and J. Graham, "Isotropic yielding in an artificially cemented soil cured under stress," *Géotechnique*, vol. 53, no. 5, pp. 493–501, 2003.

[38] D. Wang, A. Nor Edine, and R. Zentar, "Stress-dependent behavior of artificially structured and reconstituted marine soils," *International Journal of Geomechanics*, vol. 17, no. 4, article 04016103, 2017.